DEPARTMENT OF THE INTERIOR
U.S. GEOLOGICAL SURVEY

TO ACCOMPANY MAP SHEETS OF THE
CIRCUM-PACIFIC GEODYNAMIC MAP SERIES

EXPLANATORY NOTES FOR THE GEODYNAMIC MAP OF THE CIRCUM-PACIFIC REGION

by
George W. Moore

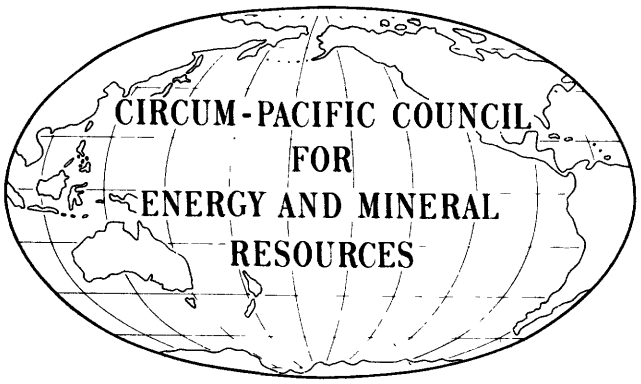

1990

CIRCUM-PACIFIC COUNCIL FOR ENERGY AND MINERAL RESOURCES
Michel T. Halbouty, Chairman and President

CIRCUM-PACIFIC MAP PROJECT
John A. Reinemund, Director
George Gryc, General Chairman

Explanatory Notes to Supplement the
GEODYNAMIC MAP OF THE CIRCUM-PACIFIC REGION

José Corvalán D.
Chairman, Southeast Quadrant Panel
Ian W. D. Dalziel
Chairman, Antarctic Panel
Kenneth J. Drummond
Chairman, Northeast Quadrant Panel
George W. Moore
Chairman, Arctic Panel
Tomoyuki Moritani
Chairman, Northwest Quadrant Panel
W. David Palfreyman
Chairman, Southwest Quadrant Panel

FREE-AIR GRAVITY ANOMALIES

Richard H. Rapp, Department of Geodetic Science and Surveying, Ohio State University, Columbus, Ohio 43210, USA

STATE OF LITHOSPHERIC STRESS

Mary Lou Zoback, U.S. Geological Survey, Menlo Park, California 94025, USA
David Denham, Bureau of Mineral Resources, Canberra, ACT 2601, Australia
Hitoshi Koide, Geological Survey of Japan, Tsukuba, Ibaraki-ken, 305 Japan
Jacques-Louis Mercier, Laboratoire de Géologie Dynamique Interne, Université de Paris-Sud, 91405 Orsay Cedex, France

EARTHQUAKE FOCAL MECHANISMS

Arthur C. Tarr, U.S. Geological Survey, Denver, Colorado 80225, USA
Frederick J. Mauk, Teledyne Geotech, 3401 Shiloh Road, Garland, Texas 75041, USA
Wilbur A. Rinehart, National Oceanic and Atmospheric Administration, Boulder, Colorado 80303, USA

HISTORICAL FAULTING

Manuel G. Bonilla, U.S. Geological Survey, Menlo Park, California 94025, USA

ACTIVE PLATE BOUNDARIES

George W. Moore, Department of Geosciences, Oregon State University, Corvallis, Oregon 97331, USA

CRUSTAL THICKNESS

David R. Soller, U.S. Geological Survey, Reston, Virginia 22092, USA
Richard D. Brown, 3501 Beta Place, Annandale, Virginia 22003, USA

CONTENTS

ABSTRACT

The Geodynamic Map of the Circum-Pacific Region consists of seven sheets and was completed in 1990. This is one of eight series of maps prepared by the Circum-Pacific Map Project that help to relate energy and mineral resources to the powerful new geologic methods and insights that have become available since the theory of plate tectonics was formulated some 25 years ago. The Geodynamic Map provides data on present-day movements of the Earth's outer layers and on stresses and density imbalances that might cause future movements. Gravity contours, incorporating newly available data based on measurements of sea-surface height by the Seasat radar altimeter, show much more detail across continental margins than on any previous map, and they accurately delineate knucklelike condyles (highs of gravity reflecting topography with a wavelength of about 300 kilometers) along the outer swells of both oceanic trenches and seamount ridges. Lithospheric stress, especially as derived from newly developed measures of systematically oriented spalling of the walls of oil wells, shows consistent maximum horizontal compression directions in plate interiors that seem more related to forces directed outwardly from spreading axes than to the absolute motions of the plates. Fault displacements during historical time indicate the present-day pattern of deformation at the surface of the Earth, and active volcanoes and earthquake first-motion directions reveal the deformation pattern from the surface to the bottoms of subduction zones, where surficial layers are inferred to penetrate most deeply into the Earth's mantle. This information plus that on crustal thickness is expected to aid in discovering the causes of the Earth's internal dynamics.

INTRODUCTION

The Circum-Pacific Map Project was established in 1973 and is producing a series of maps of the Pacific Basin and bordering parts of adjacent continents that take account of the revolutionary changes in geologic understanding that accompanied the formulation and testing of the various hypotheses that constitute the theory of plate tectonics. International in scope, the Map Project is managed by and receives input from academic, government, and industry organizations in the nations around the Pacific Basin. It is an activity of the Circum-Pacific Council for Energy and Mineral Resources, an independent international organization.

The Map Project is directed by six panels of specialists on the geology of the four quadrants of the Pacific (Northwest, Northeast, Southwest, and Southeast) and the Arctic and Antarctic regions. The general chairman of the Map Project coordinates map production from project headquarters in the offices of the U.S. Geological Survey, Menlo Park, California.

The four overlapping quadrants and the Arctic and Antarctic Sheets have a common scale of 1:10,000,000 and separate projection centers in the Lambert azimuthal equal-area projection. A seventh Lambert equal-area map at a scale of 1:17,000,000 covers the entire project area.

Eight series of maps have been published by the Map Project or are in the process of preparation and publication: Geographic, Base, Plate-Tectonic, Geodynamic, Geologic, Tectonic, Energy-Resources, and Mineral-Resources.

GEODYNAMIC MAP SERIES

The Geodynamic Series shows the present state of stress within the crust of the Earth, deformation that has occurred within historic time, and rock-density imbalances that might cause deformation in the future. The principal map elements are free-air gravity-anomaly contours, crustal thickness, earthquake focal mechanisms, direction of maximum horizontal compressive stress, active volcanoes, and faults active during historic time.

Several of the elements on the Geodynamic Map bear a close relationship to the plate boundaries that are shown in detail on the Plate-Tectonic Map of the

Circum-Pacific Region (Figure 1). In plate-tectonic theory, the Earth is considered to be covered by about 20 fairly rigid tile-like plates that move about and interact with each other along their mutual boundaries to cause earthquakes, volcanoes, and mountain chains. The plates move with respect to the body of the Earth at rates that in some places exceed 10 cm/yr, which is equivalent to 100 km/million years.

The boundaries of the major plates within the Circum-Pacific Region are printed in red on the Geodynamic Map and are identified according to whether adjoining plates (1) slide horizontally past each other at transform faults, (2) converge so that one underthrusts the other at subduction zones, or (3) rift apart to create new seafloor at spreading ridges.

Nearly all earth scientists now accept the theory of plate tectonics, and since it was put forth in a full form by Wilson in 1965, it has led to giant strides forward for the science of geology. Despite the knowledge that the plates move, and that their movement is related to geodynamic processes, we still are not certain about the ultimate cause of the movement. The Geodynamic Map sheets assemble information that is necessary in working toward a solution to this problem.

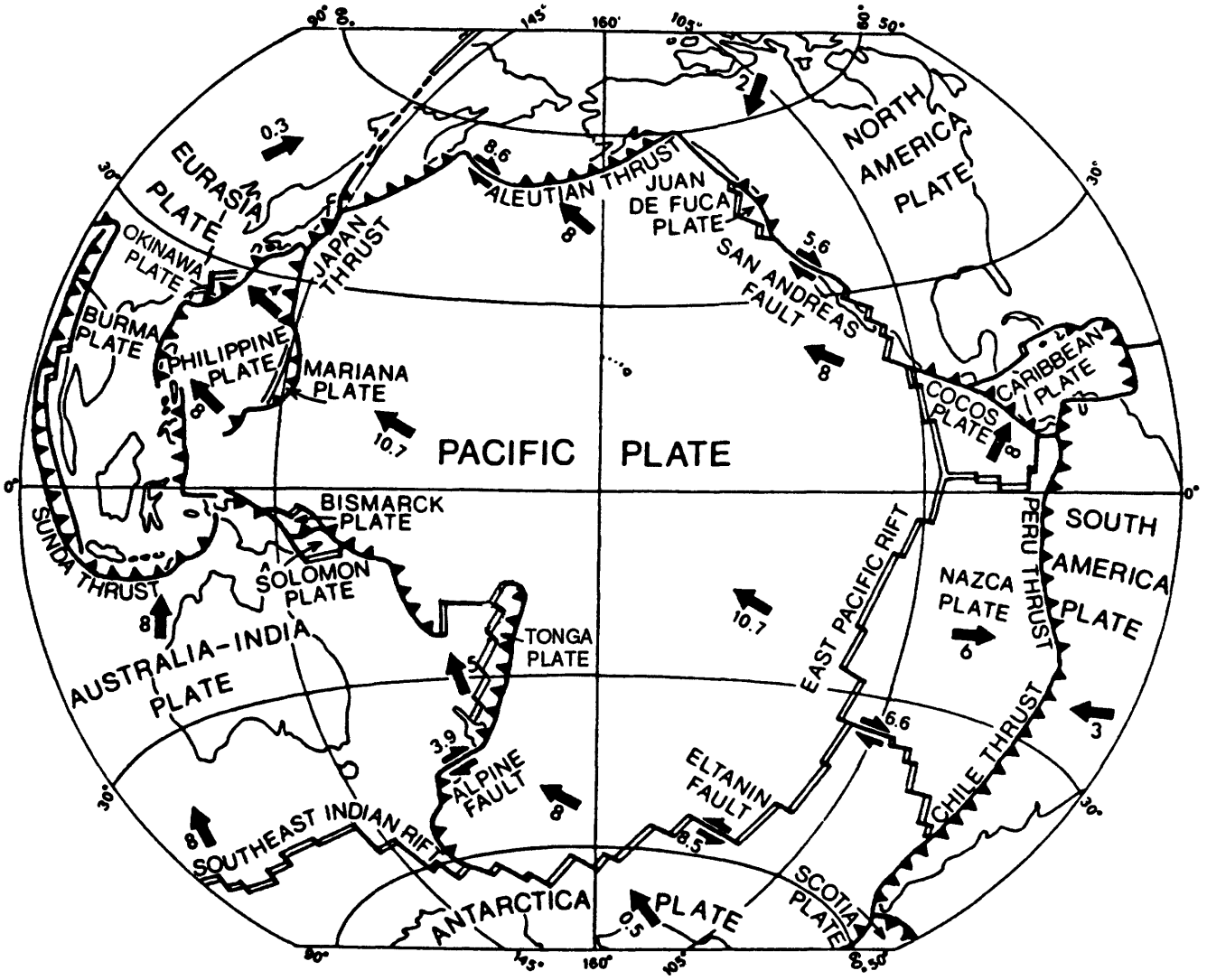

Figure 1—Tectonic plates of the circum-Pacific region. Full arrows show the direction and rate of plate movement in centimeters per year with respect to the body of the Earth, and half arrows show the relative movement between adjacent plates at major transform faults. Spreading axes appear as double lines, transform faults as single lines, and subduction zones as barbed lines on which the barbs point in the general direction that the downgoing plate moves (Moore, 1982).

FREE-AIR GRAVITY

Using evidence such as the relatively small gravitational attraction between the Earth and Moon, as indicated by the Moon's high orbit as a satellite with respect to its velocity, Newton (1687) showed that gravity decreases as the square of the distance to the attracting body. The gravity measured at any place on the surface of the Earth is dependent upon several factors, among them the distance to the center of the Earth, a latitude-dependent reduction in gravity due to centrifugal force on the spinning globe, and local mass differences within the Earth. On the free-air gravity-anomaly map, the values have been adjusted to sea level, the latitudinal effect removed, and the large average value due to the Earth's mass subtracted. The remainder consists of gravity anomalies, which are the effects of subsurface density differences.

The gravity information used for the Geodynamic Map, which has been contoured from average values for each 1-degree square of latitude and longitude (approximately 110 x 110 km near the Equator), comes from three sources: perturbations of the orbits of artificial satellites, measurements at the Earth's surface by gravimeters (very sensitive spring balances), and calculations from the height of the sea surface as measured by the Seasat satellite altimeter (Rapp, 1981).

The mapped free-air values represent the difference between the gravity at sea level and that to be expected considering the Earth as a simple ovate spheroid—an Earth flattened at the poles and bulging at the Equator because of its spin. Three factors are included in the international gravity formula to represent the shape of the spheroid and its resultant gravity field: (1) the total mass of the Earth; (2) the centrifugal effect of the Earth's spin, which causes a smaller gravity at the Equator than at the poles; and (3) a slightly greater gravity at the Equator than otherwise expected, owing to the mass of the equatorial bulge (Moritz, 1980).

Those parts of satellite orbital perturbations that are symmetric with respect to the Equator of the Earth have contributed to the international gravity formula and are therefore omitted in the derivation of gravity anomalies, whereas those parts that are nonsymmetric are retained to produce a long-wavelength part of the gravity anomalies. The Seasat determinations of sea-surface altitude were made by radar measurement of the tidally corrected distance to the surface of the ocean from a satellite of known orbit. A seamount, for example, typically is overlain by a bulge several meters high on the surface of the sea, because the mass of the seamount attracts the water laterally toward and over itself. The gravity values that have been calculated for the resulting hills and valleys of this sea-surface geoid and used to produce the gravity contours for oceanic areas are not those at the altitude of the satellite but those at the sea surface. Consequently, the Seasat and terrestrial gravity values are fully compatible, and they have been integrated on the Geodynamic Map of the Circum-Pacific Region to make a complete gravity map of all included land and sea areas.

The gravity over land areas was measured by gravimeters usually at some altitude above sea level. For the Geodynamic Map, no Bouguer correction (to remove the effect of the mass of rock between sea level and the measuring station) was subtracted, but a free-air correction for elevation (to adjust to the greater gravity at sea level, nearer the center of mass of the Earth) was made by adding the altitude times a constant to the measured gravity values.

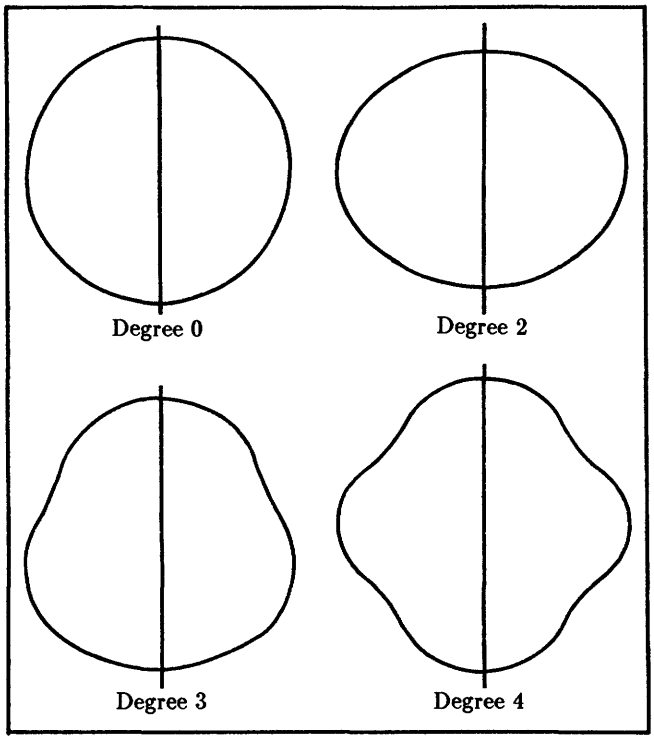

Figure 2—Low-degree spherical harmonic expansions of the type used to describe the gravity field of the Earth. The inset maps on the Geodynamic Map sheets use Degree 10 (100 smoothly contoured undulations on the Earth), and the main map uses Degree 180 (64,800 undulations).

Although the gravity at a terrestrial station can be measured with respect to a reference station and to the international spheroid, the Seasat anomalies initially are not referenced to the spheroid, so they must be adjusted to the Earth using all available gravity information. This is done by a spherical harmonic analysis in which simple and then successively more complex but regular sets of undulations on the Earth are used to adjust successively shorter wavelengths of gravity data (Figure 2).

In the spherical harmonic analysis, wavelengths superimposed on the geoid and on the global gravity field are identified by a notation system that uses the term degree along with numerals. Degree 0 refers to the mass of the Earth considered as a sphere, degree 1 to a bulge on one side of the sphere (not present on the real Earth, which is rotationally symmetrical), degree 2 to the equatorial bulge, degree 3 to a pear-shaped Earth,

degree 4 to a midlatitude gravitational low caused by a decline in the gravitational attraction due to the equatorial bulge with distance from it, and various higher degrees to shorter-wavelength density imbalances within the Earth. The degrees are accompanied by families of orders, also numbered, that expand the wavelengths into two-dimensional arrays on the surface of the Earth. Coefficients for each degree and order indicate the magnitude of the anomalies for that wavelength.

To determine the free-air gravity patterns on the Circum-Pacific Geodynamic Map, coefficients have been used to degree and order 180, giving 64,800 data points, one for each 1-degree square of latitude and longitude on the surface of the Earth. For the small-scale degree-10 inset maps on the map sheets, coefficients for all degrees higher than 10 have been taken to be zero, allowing for 100 smoothed data points on the surface of the Earth.

The main (degree-180) map shows details of the gravity field of many oceanic areas for the first time. Also, the gravity information shown across continent-ocean boundaries is much improved over previous maps.

Because gravity decreases as the square of the distance to the attracting body, a small density imbalance at shallow depth in the Earth can cause the same departure from the expected surface gravity as a large deep imbalance, but the anomaly from the deeper source will have a longer wavelength. For example, on the small degree-10 map, which has anomaly wavelengths of about 2,000 km and longer, an anomaly could reflect an undulation on the surface of the Earth's core at a depth of 2,900 km, where the core-mantle density contrast is about 4 grams/cubic centimeter. Alternatively, the anomaly could be caused by shallower density contrasts within the mantle at subducted plate slabs or at low-density plumes of warm material in mantle convection cells, where the density contrast is less than 1 g/cm^3. On the main degree-180 map, the anomalies have minimum wavelengths of about 200 km and are insensitive to the details of short-wavelength changes in gravity near the surface. They reflect density variations most clearly at a depth that is of the order of their minimum wavelength, within the lower crust and upper mantle.

Conspicuous features shown by the map are the deep gravity lows at oceanic trenches (Vening Meinesz, 1929) and the gravity highs over islands and mountains of the adjacent volcanic arcs. A similar edge effect appears at rifted continental margins, such as those around Australia and Antarctica and along the east coast of the Americas. At rifted margins, a gravity low is present along the base of the continental slope because of the mass deficiency in the nearby thick crust of low density that underlies the adjacent continent. A complementary gravity high is present along most lengths of the continental shelf for the opposite reason: nearness to the dense mantle that at shallow depth underlies the thin oceanic crust. But this marginal gravity high is decreased where areas of low gravity caused by sedimentary basins intersect the rifted margin. By removing the edge effects along such margins, the continental gravity fields of formerly contiguous areas can help to match continents such as Australia and Antarctica that have drifted apart.

Gravity lows follow moat-like troughs that surround seamounts and midocean ridges such as the Hawaiian Ridge (Watts, 1982). The fact that such moats encircle these large loads on the Earth's crust at a distance of about 150 km, somewhat analogously to the sag around a skater on an ice-covered pond, has long indicated that the Earth consists of a strong but flexible outer layer overlying a weak layer at depth. Reasoning from evidence of this sort led Barrell (1914) to recognize and name the asthenosphere as the weak layer that underlies the rigid lithosphere.

Throughout the map, linear gravity highs mark seafloor swells or arches seaward from and parallel to oceanic trenches and seamount troughs. These swells are a consequence of the effectively fluid asthenosphere buoying up the flexurally rigid lithosphere. Where bent lithosphere is held down by the load of a ridge on one side of a trough, buoyancy lifts an outboard belt of lithosphere on the other side of the trough to create a seafloor bulge.

Another feature related to the ridge-trough-swell combination is seen clearly on the map. In the gravity and regional bathymetry, knucklelike humps, here named condyles, are distributed along the lengths of the outer swells of both trenches and seamount troughs. The condyles have an average wavelength of about 300 km. Independent evidence, based on shipboard gravity surveys at a few well-mapped outer swells such as that of the Aleutian Trench (Bowen et al, 1981), prove that the condyles are real features of the Earth's gravity field. Two mechanisms that might have produced the condyles are thermal convection cells below the lithosphere and folding along the axes of the swells at a wavelength related to the flexural rigidity of the lithosphere.

The high gravity values at the condyles generally lie next to especially low values at the adjacent troughs and trenches. Hence linear gravity highs do not extend out at right angles to the swells, but the highs and lows form a roughly equidimensional checkerboard or honeycomb pattern. One possibility is that this pattern is related to the hexagonal Bénard convection pattern that forms when a horizontal layer of fluid is heated from below and cooled from above (Richter and Parsons, 1975). A Bénard convection cell generally is equidimensional in vertical cross section, and upwelling and sinking occur at opposite sides of each cell. Two cells, therefore, would be required to produce the 300-km wavelength in the overlying layer, leading to a thickness of the hypothetical convecting layer of about 150 km.

The condyles have about the same average wavelength as the sets of ridges, trench-troughs, and outer swells, and this fact may be a further indication of a characteristic wavelength for the flexurally rigid lithosphere. The same wavelength also is observed for onshore sedimentary basins and for island groups along volcanic ridges, although the spacing of individual erup-

tive centers is less. Horizontal stresses within the lithosphere and deformation related to plate movement, particularly where the lithosphere deforms viscoelastically, may lead naturally to a two-dimensional array of gravity anomalies with a wavelength of about 300 km. On the Geodynamic Map this pattern seems to be particularly well developed where the lithosphere is strongly bent at oceanic trenches and midplate volcanic ridges.

CRUSTAL THICKNESS

The concept that the Earth has a crust dates from a time when lava erupting from volcanoes led people to think that molten rock underlies the surface everywhere at shallow depth. Later the crust came simply to represent familiar surface rocks with an average density of 2.7 g/cm^3, known to be lighter than those below because from angular-momentum calculations the Earth has an average density of about 5.5 g/cm^3. In 1910, Mohorovičić discovered that seismographs more than about 200 km from an earthquake detect a seismic wave that arrives before the wave received first at closer stations. The faster wave travels down to the mantle, moves horizontally through it at a high speed, and then travels up to the surface again. Despite its longer path, it arrives before a wave that takes the more direct but slower route through the less dense crust. The boundary between the crust and mantle, now known as the Mohorovičvić discontinuity or moho, is marked by an increase in seismic velocity from about 6.9 km/s to 8.1 km/s. The moho is an important compositional and velocity interface within the lithosphere. It usually lies at some distance above the boundary of the lithosphere and the asthenosphere, which is a viscosity transition but probably not a major compositional boundary.

The former Mohole Project was conceived to drill through and sample the crust-mantle boundary to determine the reason for its large change in seismic velocity. At about the time the Mohole Project was scrapped because of skyrocketing costs (to be replaced by the more modest but superlatively successful Deep Sea Drilling Project), short segments of the moho were recognized cropping out on land (Hess, 1965). In areas of continental collision, mantle material of the upper plate may be lifted to the surface where underthrust by buoyant continental crust. In such places the moho is identified as a boundary between gabbro of the crust and peridotite of the mantle. Laboratory studies show that the seismic velocities of these rocks correspond well with the velocities that had been measured at depth by Mohorovičić.

Natural earthquakes were originally used to determine crustal thickness, but later these were largely supplanted by artificial explosions, which can be accurately positioned and timed. Mohorovičić's seismic-refraction method, in which a spaced set of seismic receivers is used to determine the depth to the velocity discontinuity, is now being augmented by the seismic-reflection method, in which echoes from the crust-mantle boundary are processed in much the same way that an echo sounder plumbs the seafloor. The Geodynamic Map mainly uses seismic-refraction values supplemented in remote areas by values from earthquake surface waves, in which crustal thickness is determined from characteristic plots of velocity versus frequency for seismic waves traveling in the crustal layer (Jeffreys, 1925).

Crustal thickness is shown by insets on the 1:10,000,000 sheets of the Geodynamic Map, updated from a global compilation that utilized 2508 crustal thickness values from 297 published papers (Soller et al, 1982). On the average, the crust is about 35 km thick under the continents and 6 km thick under the ocean basins. Until recently, seismic-reflection profiling to show the moho across continent-ocean boundaries had been difficult, but profiles near Antarctica (where the ice cap onshore protected against erosion and thereby led to a very thin sediment cover offshore) show that the moho deepens rather smoothly from oceanic to continental levels (Eittreim et al, 1984).

Crustal thickness under the ocean basins is fairly uniform, and those departures from normal values that do occur are useful in geodynamic interpretation. On land, areas of thin crust are present near continental margins and at places that have been suggested as sites of incipient continental rifting. Areas of thick crust occur along mountain ranges and at places where former continental collision has been inferred. The crustal-thickness maps provide a ready reference for interpreting the geodynamic significance of the other map elements in this map series.

EARTHQUAKE FOCAL MECHANISMS

When rocks suddenly slip along a fault to relieve stresses within the Earth, earthquake waves result that can be recorded at distant seismographs. These waves contain useful information about the direction of slip and can be analyzed to provide valuable insights into geodynamic processes at the focus of the earthquake.

Reid (1910) developed the now generally accepted elastic-rebound theory of earthquakes. During a long period of slow rock deformation, elastic strain builds up between rock masses on opposite sides of a fault. Slip at the fault is prevented by friction until a critical threshold of strain is exceeded. Then the rocks snap past each other along the fault to release some of the stored energy.

The first motion received at a distant seismograph takes one of two forms. If the earthquake-affected rocks producing the first motion move toward the seismograph, the stylus of the seismograph is deflected so as to

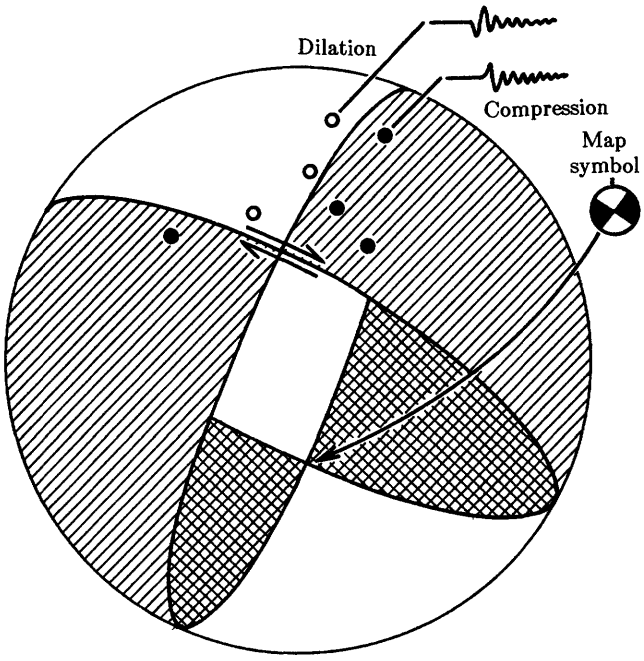

Figure 3—Diagrammatic zones of compressive and dilational first motions on the Earth from an earthquake on a vertical right-lateral strike-slip fault, as determined by the first motions recorded at scattered seismograph stations. The sphere can also represent the directional distribution of compression and dilation at the earthquake focus, and the first-motion symbol is derived from its lower hemisphere.

indicate compression. If the rocks move away, the stylus is deflected in the opposite direction to indicate dilation.

Whether compression or dilation is recorded at seismographs at various positions around an earthquake depends on the direction from the focus (Nakano, 1923). The first motions divide into four quadrants on the surface of the Earth, two for each side of the fault (Figure 3). One set of diagonally opposite quadrants includes all seismograph stations toward which the rocks first moved during the earthquake, and the other, all stations from which the rocks moved away.

The four quadrants are defined by two mutually perpendicular planes that pass through the focus of the earthquake. One of these is an extension of the surface that ruptured during the earthquake (Byerly, 1926). Which one this is can usually be determined by comparison with the trend of faults mapped nearby on the ground or by inference from an expected stress field, such as near a plate boundary with a previously known pattern of movement.

The four first-motion quadrants for each earthquake define a sphere that is represented on the Geodynamic Map by a circular symbol drawn as a plan view of a stereographic projection of the sphere's lower hemisphere (Tarr and Mauk, 1983). Dilational quadrants are uncolored, compressional quadrants are colored, and the colors are keyed to the depth of focus of the earthquake.

This focal-mechanism symbol can be visualized as the inside of a bowl in which the quadrant boundary that marks the fault is the intersection of the fault plane with the inner wall of the bowl. A centered straight quadrant boundary defines the trend of a vertical fault. A nearly centered boundary represents a steep fault, whereas a strongly curved boundary near the edge of the symbol represents a gently dipping fault. A boundary that is convex toward the left represents a west-dipping fault; one toward the right, east-dipping.

Different orientations of the symbols represent different classes of faults: a centered junction of the four quadrants denotes strike-slip faulting; a central colored quadrant, thrust faulting; a central uncolored quadrant, normal faulting; and an intermediate pattern, oblique-slip faulting (Figures 3 and 4).

The direction of compression or tectonic transport at a fault can be inferred from the focal mechanism symbol as a direction passing from an uncolored dilational quadrant into and through a colored compressional quadrant. Hence, on a vertical northwest-trending strike-slip fault, right-lateral slip, in which the side of the fault opposite from the viewer is displaced toward the right, is represented by a symbol on which the quadrant boundaries form an X at the center, and the west and east quadrants are colored (Figure 3).

During the development of the theory of plate tectonics, seismology has supplied important data to define the boundaries of the plates and to help indicate directions of plate movement (Isacks, Oliver, and Sykes,

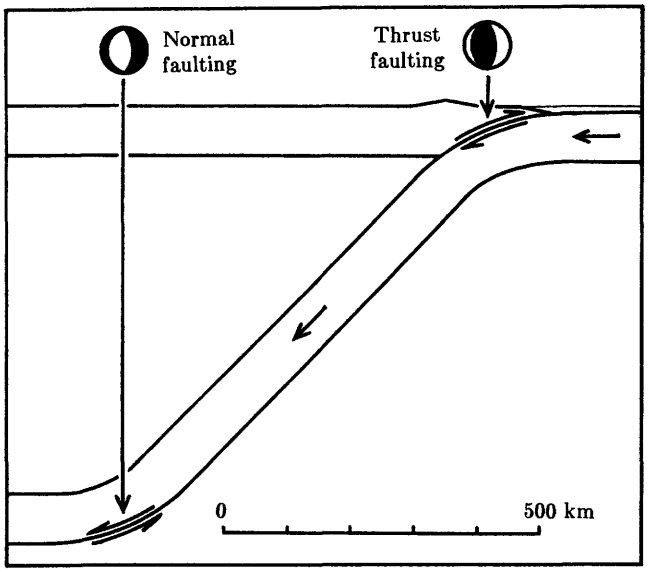

Figure 4—Schematic cross section of a convergent plate boundary (subduction zone), showing typical first motions of earthquakes. Shallow-focus and intermediate-focus earthquakes at subduction zones usually originate from thrust faulting, whereas deep-focus earthquakes are commonly observed to originate from normal faulting. A possible cause is an increased rate of shear at the outside of bends in the subducting lithospheric slab.

1968). Earthquake focal mechanisms still remain the principal evidence for the downward motion of plates at subduction zones (Minster and Jordan, 1978).

On the Geodynamic Map, the focal-mechanism symbols are generally compatible with inferred plate movements, but some exceptions occur, especially near complex plate boundaries and intersections. Strike-slip symbols, with the proper sense of movement, mark transform faults that delineate horizontal slip between adjacent plates. At seafloor-spreading axes, earthquakes of magnitude 5.5 (the lower limit used for the map) are rare or absent, because sufficient stress cannot build up in the thin hot crust. Consequently, symbols for normal faults, such as would be expected in an extensional regime, are absent. Instead, strike-slip symbols identify short transform faults in nearby cooler crust that offset the spreading axes and mark their approximate positions.

Recurrent shallow and intermediate thrust faulting at the edge of the upper plate clearly defines subduction zones. Nearly all investigators assume that this pattern results when the downgoing plate shears against the overriding plate (Figure 4). Opinion diverges, however, as to the nature of the predominant driving mechanism. Does the slab-like downgoing plate sink gravitationally within the subduction zone by what has been called slab-pull, does it move forcefully into the subduction zone because of motion generated in the vicinity of a spreading ridge by what has been called ridge-push, or is the driving force some other mechanism such as viscous drag of moving asthenosphere?

Deep earthquakes at subduction zones usually do not possess the thrust-faulting first motions that characterize the shallow and intermediate earthquakes. Deep earthquakes emanate from normal faulting in which an upper block moves downward with respect to a lower block. Some investigators have interpreted this pattern to indicate extension, and they have therefore taken it as supporting evidence for a significant component of slab-pull at subduction zones. We should keep in mind, however, that a normal-faulting mechanism indicates only that the slab or part of it is moving downward with respect to underlying material. Such movement could be caused equally well by push on the slab from above.

Normal faulting is common at the outer swells of oceanic trenches, a fact that would be compatible either with slab-pull or with stretching at the convex outer curves of the downgoing plates as they bend down into subduction zones. By contrast, the rare earthquakes that occur in the middle of an oceanic plate g[illegible] have thrust-faulting first motions. These indicate [illegible] midplate regions are under compression, a fact that tends to support those hypothetical plate-driving mechanisms that involve ridge-push and viscous drag by the asthenosphere on the lithosphere.

STATE OF LITHOSPHERIC STRESS

In addition to information from earthquake focal mechanisms, several other kinds of measurements and observations reveal the orientation of present-day stresses within the Earth that might cause future faulting and rock deformation. Stress indicators that are plotted as symbols in separate colors on the Geodynamic Map include grooves and scratches on polished fault surfaces (slickensides) formed during the present (Quaternary) geologic period, alignment of Quaternary volcanoes, artificially induced hydraulic fracturing in boreholes, borehole overcoring, and well ellipticity (Zoback and Zoback, 1980).

The free face at the surface of the Earth causes the axis of maximum stress within the upper crust to be oriented either vertically or horizontally (Figure 5). On the Geodynamic Map, opposing arrows indicate the maximum horizontal compressive stress direction at specific localities. The traces of thrust faults and fold axes tend to lie perpendicular to these arrows, those of normal faults and rifts parallel to them, and those of strike-slip faults at intermediate angles.

Slickensides indicate the direction of slip during the faulting that formed them. Several sets of slickensides on nonparallel surfaces that can be inferred to have formed under a given stress field and which seem young enough to reflect the present state of stress in the Earth can be used to determine the direction of maximum horizontal compression (Mercier, 1981). In a few places on the Geodynamic Map, these Quaternary slickenside data points are supplemented by symbols in the same color for stress directions determined from slight offsets measured on intersecting sets of rock joints (Lockwood and

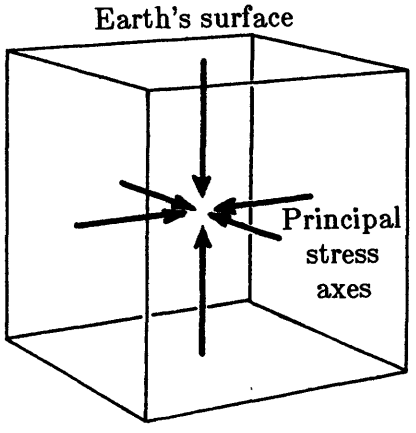

Figure 5—Diagram showing orientation of the maximum, intermediate, and minimum principal stress axes in the upper crust. One of these axes is usually perpendicular to the Earth's surface, a free face. Thrust faults usually trend perpendicular to the maximum horizontal compressive stress axis, normal faults parallel with it, and strike-slip faults at intermediate angles.

Moore, 1979).

If several young volcanoes of the same age erupt along a linear belt, they are inferred to have formed along a break at depth that was forced to allow magma to pass. Such magmatic fractures, caused by the injection of molten rock under high pressure, are oriented parallel to the maximum horizontal compressive stress direction, because opening of fractures in other directions is restrained by the compression (Nakamura, 1977). Igneous dikes show a similar relationship to horizontal stress axes, and they are particularly useful for revealing past states of stress. In general, however, they have not been used on the Geodynamic Map of the Circum-Pacific Region, because the time required to expose them by erosion is long enough that they are likely to record a stress field different from that of the present.

Hydraulic fracturing, commonly used to increase the permeability of producing formations in oil and gas wells, is induced by pumping in a fluid and sand at high pressure so as both to create new openings and to hold them open when the pressure is released. The fractures that form, as with magmatic fracturing, generally are vertical and parallel to the maximum horizontal compressive stress direction. Their orientations are determined either by an inflatable packer that can take an imprint of the wall of the hole or by a video or sonic image of the borehole. Hydraulic-fracturing arrow symbols on the Geodynamic Map are plotted parallel to vertical fractures opened in this way.

One of the oldest methods of in-place determination of lithospheric stress is borehole overcoring. In one form of this method, a small pilot hole is drilled into the bottom of a larger hole, and a cell containing a set of strain gauges is inserted (Denham et al, 1980). The pilot hole and strain gauges are then overcored by a larger diameter core barrel. The core, which had previously been deformed by the natural lithospheric stress, relaxes after the overcoring and changes shape. When it is brought to the surface, the displacement measured by the the strain gauges indicates the orientation of the lithospheric stress. Most holes of this sort are drilled for scientific purposes, and they tend to be shallow because of high drilling costs. Shallow in-place stress measurements are greatly affected by local topographic irregularities, so borehole-overcoring data usually have larger errors than other determinations of lithospheric stress. On the Geodynamic Map, borehole-overcoring information has been used only where other types of stress measurements are scarce or absent.

In the past few years, an exciting new body of lithospheric-stress data has become available. In 1970, Cox noticed that four-arm caliper logs of oil wells within a given region show the cross sections of the wells to have a systematically oriented ellipticity. Regardless of the age or dip of the beds, or of the trends of structures in the region, wells develop a consistent pattern of breakout or spalling of rock material at opposite sides of the hole during the drilling process. Bell and Gough (1979) suggested that the long axis of the elliptical cross section lies at right angles to the maximum horizontal compressive stress, because the rock would tend to spread laterally and spall off into the hole in that direction from both sides. Orientations of well ellipticity agree nicely with other local measurements of lithospheric stress, and caliper logs are available from oil fields in many parts of the Circum-Pacific region. The abundance of this kind of data and the fact that it is available in deep wells that are not influenced by surface topographic effects make it particularly useful for geodynamic studies.

The information on lithospheric stress from all these methods, plus that from earthquake focal mechanisms, shows fairly consistent patterns in the interiors of the continents. Over a large area of the midcontinent of North America, for example, the maximum horizontal compressive stress direction trends northeasterly (Zoback and Zoback, 1980). This direction is parallel to the direction of absolute motion of the North America plate as inferred by Minster and Jordan (1978) from global plate interactions and from lines of seamounts inferred to have come from fixed magma sources (hotspots) below the plates (Figure 1). It is uncertain, however, whether this parallelism with the absolute direction of plate motion derives from cause and effect or from chance. Australia shows a rather consistent maximum horizontal compressive stress direction that is at right angles to the direction of plate movement. The information presented on the Geodynamic Map suggests that the stress may be related to plate-boundary interactions, but at this time it seems unlikely to be coupled to the absolute motion of the individual plates.

VOLCANIC CENTERS

The behavior of the interior of the Earth is assumed to have been reasonably uniform during the Holocene Epoch (the past 10,000 years). Therefore, volcanoes that have been active during the Holocene are inferred to indicate present-day subsurface processes and are plotted on the Geodynamic Map (Simkin et al, 1981). In a plate-tectonic context, most volcanoes form in one of three geodynamic settings: (1) along lines of rifting at spreading axes or incipient spreading axes; (2) at volcanic arcs above subduction zones; and (3) on midplate volcanic ridges that are inferred to overlie hotspots.

Soon after the idea of seafloor spreading was put forth, Green and Ringwood (1963) formulated the concept that a partial melting of the Earth's mantle material produces basaltic lava. Basalt, and its coarsely crystalline equivalent gabbro, are considered to be effusions from the dense peridotite of the mantle, and they form the 6-km-thick crust of the ocean basins. Only rarely does the basalt along an oceanic spreading axis become so thick that the top of an active volcano is exposed above the sea surface. In areas of continental rifting, however, subaerial basaltic volcanoes have been

rather common in geologic history.

Marshall (1912) recognized that the andesite and related rocks typical of volcanoes at island arcs can be distinguished both geographically and chemically from the basaltic lavas found in the middle of the oceans. The low-density and light-colored andesitic rocks, abundant at volcanoes along both island arcs and continental margins, have become, together with deep-focus earthquakes, the principal means for recognizing convergent plate boundaries. These rocks clearly derive from partial melts of material at depth, but it is a matter of controversy whether that material is basalt in subducted lithospheric slabs or deep mantle material whose melting is facilitated by the fluxing action of water carried down within the slabs. Whatever the source material, volcanic-arc magmatism is an important means by which the continental crust is built up.

Basaltic volcanoes at midplate islands such as Hawaii are used to identify the absolute motion of the lithospheric plates—that is, the motion with respect to the body of the Earth. In theory, the magma of such a hotspot volcano originates from a fixed sublithospheric source, so that as the plate moves over it a line of new volcanic islands extends in the direction of plate motion. Evidence supporting this fixed-hotspot theory consists of the compatibility with directions of plate motion indicated by earthquake first motions at subduction zones and the internal consistency in direction between several hotspot traces on the same plate.

The topographic relief of hotspot islands and seamounts declines toward the older end of hotspot traces, suggesting that the hotspots once lay at the crests of spreading axes. The hotspot traces usually meet the former ridge crests at the positions of long transform faults or at former triple junctions, places where three spreading axes once intersected. At this time we do not know whether the hotspots caused the spreading axes to form, or whether the existence of the long transform faults and triple junctions led to the steady production of basalt at the hotspots.

HISTORICAL FAULTING

Perhaps the most convincing demonstrations that the Earth is a dynamic planet are the surface ruptures and rock offsets that often accompany major earthquakes. Approximately 110 examples of faulting recorded during historical time are plotted on the Geodynamic Map. Along some plate boundaries, people have observed faulting several times over the years at the same place, usually with the same sense of displacement.

Historical faulting has been reported most commonly in areas of especially frequent earthquakes. Surface offset has rarely been described for earthquakes with a Richter magnitude of less than 5, because the displacement accompanying them is so small (less than about 2 cm) that it is usually concealed by soil. Both fault offset and rupture length show a systematic relationship to earthquake surface-wave magnitude (Figure 6). A magnitude 6 earthquake, for example, typically accompanies a fault offset of about 20 cm and a rupture length of 4 km, whereas a magnitude 8 earthquake has a fault offset of 10 m and a length of 300 km (Bonilla et al, 1984). Nevertheless, many moderate and even some great earthquakes produce no surface trace, because the rupture area is on a deep fault plane that does not intersect the Earth's surface.

Most plate boundaries lie beneath the sea, and historical faulting usually is not reported for them. Transform-fault boundaries on land, however, such as the San Andreas fault in California, provide a clear record of repeated displacement throughout the period of historical time. Zones of continental extension, such as the Basin-and-Range province of the western United States (an area of possible future seafloor spreading), are broad belts with multiple sites of historical faulting. Wide zones of faulting also occur where a plate boundary changes along its length from a subduction zone to a transform fault, as at North Island, New Zealand. There, seafloor sediment, like that being subducted at the Tonga Trench and adjacent trenches, accumulates as thrust sheets at the north end of the Alpine strike-slip fault system, where subduction cannot occur (Moore, 1983).

The most impressive faulting of all takes place in areas of continental collision. The Earth's preeminent

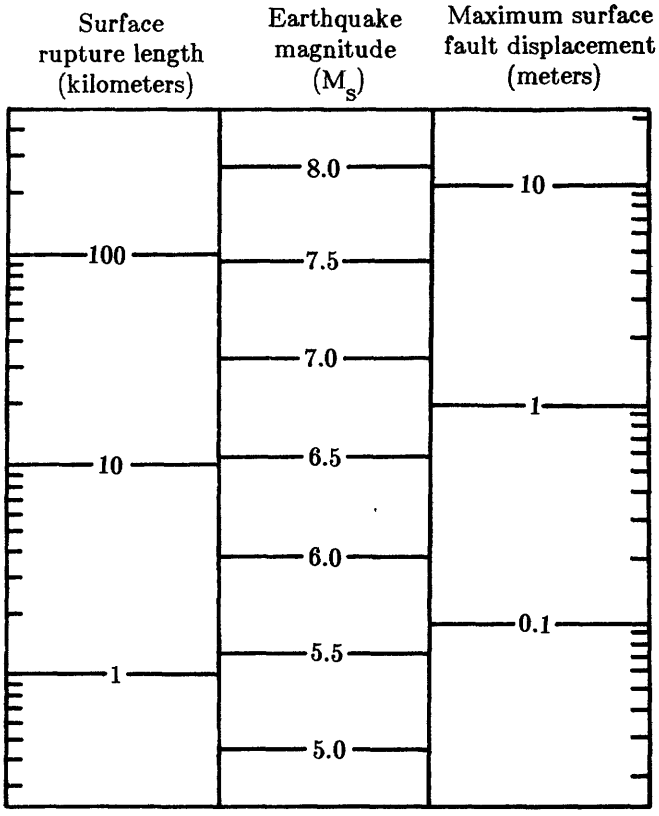

Figure 6—Approximate relationship between fault rupture length, earthquake magnitude, and fault displacement (adapted from Bonilla, Mark, and Lienkaemper, 1984).

collision zone lies along the Himalayas, where India drives against Eurasia at the great Indus suture zone, and compression and underthrusting have created the Tibetan Plateau. Adjacent and parallel to the join between these continental masses, a series of arcuate thrust faults has cut through southwestern China during historical time (Molnar and Deng, 1984). As the continental crust under Tibet became stacked to its present thickness of 80 km—the thickest in the world—southwest-dipping faults have broken through the upper plate. The effect of the collision may be felt more than 3,000 km away, at Lake Baikal in Siberia, where a series of movements related to the northeastward thrust of India seems to have rifted open the lake basin, and historical faulting indicates active left-lateral shear against the more stable part of the Eurasian plate to the northwest.

Historical faulting and the eruption of volcanoes furnish vivid illustrations of the Earth's dynamic internal energy. Information about these and their distribution, combined in this map series with quantitative measures of gravity, crustal thickness, earthquake mechanisms, and lithospheric stress, provide resources for new research into the causes and modes of action of that energy.

ACKNOWLEDGEMENTS

For help in preparing these notes on the Geodynamic Map of the Circum-Pacific Region, I am indebted to the authors of the individual map elements, who are listed on page 2. The manuscript was reviewed by Warren O. Addicott, Campbell Craddock, Michael A. Fisher, Ellen J. Moore, and Peter H. Stauffer.

REFERENCES CITED

Barrell, J., 1914, The strength of the Earth's crust: Journal of Geology, v. 22, p. 28-48, 145-165, 209-236, 289-314, 441-468, 537-555, 655-683, 729-741.

Bell, J. S., and D. I. Gough, 1979, Northeast-southwest compressive stress in Alberta: evidence from oil wells: Earth and Planetary Science Letters, v. 45, p. 475-482.

Bonilla, M. G., R. K. Mark, and J. J. Lienkaemper, 1984, Statistical relations among earthquake magnitude, surface rupture length, and surface fault displacement: Seismological Society of America Bulletin, v. 74, p. 2379-2411.

Byerly, P., 1926, The Montana earthquake of June 28, 1925: Seismological Society of America Bulletin, v. 16, p. 209-263.

Bowen, C., W. Warsi, and J. Milligan, 1981, Free-air gravity anomaly map of the world: Geological Society of America Map and Chart Series, MC-45, scale 1:22,900,000.

Cox, J. W., 1970, The high resolution dipmeter reveals dip-related borehole and formation characteristics: Society of Professional Well Log Analysts, 11th Annual Symposium, 25 p.

Denham, D., L. G. Alexander, and G. Worotnicki, 1980, The stress field near the sites of the Meckering (1968) and Calingiri (1970) earthquakes, Western Australia: Tectonophysics, v. 67, p. 283-317.

Eittreim, S. L., M. A. Hampton, J. R. Childs, and G. W. Moore, 1984, The East Antarctic passive margin: structure and stratigraphy across its continent-ocean boundary: Eos (American Geophysical Union Transactions), v. 65, p. 1105.

Green, D. H., and A. E. Ringwood, 1963, Mineral assemblages in a model mantle composition: Journal of Geophysical Research, v. 68, p. 937-945.

Hess, H. H., 1965, Mid-ocean ridges and tectonics of the sea-floor, *in* W. F. Whittard and R. Bradshaw, eds., Submarine geology and geophysics: London, Butterworths, p. 317-332.

Isacks, B., J. Oliver, and L. R. Sykes, 1968, Seismology and the new global tectonics: Journal of Geophysical Research, v. 73, p. 5855-5899.

Jeffreys, H., 1925, On the surface waves of earthquakes: Royal Astronomical Society Monthly Notices, Geophysical Supplement, v. 1, p. 282-292.

Lockwood, J. P., and J. G. Moore, 1979, Regional extension of the Sierra Nevada, California, on conjugate microfault sets: Journal of Geophysical Research, v. 84, p. 6041-6049.

Marshall, P., 1912, The structural boundary of the Pacific basin: Australasian Association for the Advancement of Science Report, v. 13, p. 90-99.

Mercier, J.-L., 1981, Extensional-compressional tectonics associated with the Aegean arc: comparison with the Andean cordillera of south Peru—north Bolivia: Royal Society of London Philosophical Transactions, ser. A, v. 300, p. 337-355.

Minster, J. B., and T. H. Jordan, 1978, Present-day plate motions: Journal of Geophysical Research, v. 83, p. 5331-5354.

Mohorovičić, A., 1910, Das Beben vom 8.X.1909: Zagreb Meteorologisch Observatorium Jahrbuch 1909, v. 4, p. 1-63.

Molnar, P., and Deng Q., 1984, Faulting associated with large earthquakes and the average rate of deformation in central and eastern Asia: Journal of Geophysical Research, v. 89, p. 6203-6227.

Moore, G. W., 1982, Plate-tectonic map of the circum-Pacific region explanatory notes: Tulsa, Okla., American Association of Petroleum Geologists, 14 p.

Moore, G. W., 1983, Structural dynamics of the shelf-slope boundary at active subduction zones: Society of Economic Paleontologists and Mineralogists Special Publication 33, p. 97-105.

Moritz, H., 1980, Geodetic Reference System 1980: Bulletin Geodesique, v. 54, p. 395-405.

Nakamura, K., 1977, Volcanoes as possible indicators of tectonic stress orientation—principle and proposal: Journal of Volcanology and Geothermal Research, v. 2, p. 1-16.

Newton, I., 1687, Philosophiae naturalis principia mathematica: London, J. Streater, 510 p.

Nakano, H., 1923, Notes on the nature of forces which give rise to the earthquake motions: Japan Central Meteorological Observatory Seismological Bulletin, v. 1, p. 92-120.

Rapp, R. H., 1981, The Earth's gravity field to degree and order 180 using Seasat altimeter data, terrestrial gravity data, and other data: Ohio State University Department of Geodetic Science and Surveying Report No. 322, 53 p.

Reid, H. F., 1910, The mechanics of the [San Francisco] earthquake: Carnegie Institution of Washington Publication 87, v. 2, 192 p.

Richter, F. M., and B. Parsons, 1975, On the interaction of two scales of convection in the mantle: Journal of Geophysical Research, v. 80, p. 2529-2541.

Simkin, T., L. McClelland, D. Bridge, C. Newhall, and J. H. Latter, 1981, Volcanoes of the world: Stroudsburg, Pennsylvania, Hutchinson Ross, 232 p.

Soller, D. R., R. D. Ray, and R. D. Brown, 1982, A new global crustal thickness map: Tectonics, v. 1, p. 125-149.

Tarr, A. C., and F. J. Mauk, 1983, A global compilation of earthquake focal mechanisms: U. S. Geological Survey unpublished manuscript, 13 p.

Vening Meinesz, F. A., 1929, Theory and practice of gravity measurements at sea: Delft, Waltman, v. 1, 95 p.

Watts, A. B., 1982, Tectonic subsidence, flexure and global changes of sea level: Nature, v. 297, p. 469-474.

Wilson, J. T., 1965, A new class of faults and their bearing on continental drift: Nature, v. 207, p. 343-347.

Zoback, M. L., and M. D. Zoback, 1980, State of stress in the conterminous United States: Journal of Geophysical Research, v. 85, p. 6113-6156.